RSC Advances

ROYAL SOCIETY OF CHEMISTRY

www.rsc.org/advances

Effects of post-treatment on the structure and properties of PVDF/FEP blend hollow fiber membranes

Qing-lin Huang*, Yan-jie Wu,Chang-fa Xiao, Kai-kai Chen, Liang Song, Zhen Liu

(State Key Laboratory of Separation Membranes and Membrane Processes, Department of Material Science and Engineering, Tianjin Polytechnic University, Tianjin, China, 300387)

Abstract: Polyvinylidene fluoride (PVDF)/poly(tetrafluoroethylene-co-hexafluoropropylene) (FEP) blend hollow fiber membranes were prepared by the melt-spinning method.The effects of drawing conditions (drawing ratio andtemperature) on the structure and properties of the membraneswere investigated bydifferential scanningcalorimetry (DSC),dynamic mechanical analysis (DMA), and analysis of membrane morphology.The storage modulus increased with increasingdrawingtemperature at the same drawing ratio, which improvedthemembrane's elasticity. The quantity and pore size of the interfacial microvoidsboth increasedsignificantly with an increase in thedrawing ratio at the same drawing temperature. Finally, themembranes were evaluated for their performance in vacuum membrane distillation (VMD).All membranes had asalt rejection higher than 99.0%.

Keywords:polyvinylidene fluoride (PVDF); poly(tetrafluoroethylene-co-hexafluoropropylene) FEP; hollow fiber membrane; membrane distillation (MD); drawing

This manuscript has been thoroughly edited by a native English speaker from an editing company. Editing Certificate will be provided upon request.

*Correspondence to: Qinglin Huang, Doctor. Address: 399 Binshui West Street, Xiqing District, State Key Laboratory of Separation Membranes and Membrane Processes, Tianjin Polytechnic University, Tianjin, P.R.China (E-mail: huangqinglin@tjpu.edu.cn), Tel:+86 022 83955794, Fax: +86 022 83955055

1. Introduction

Poly(vinylidene fluoride) (PVDF) has excellent chemical resistance, physical and thermal stability, high strength, and flexibility that make it one of the most important polymeric membrane materials [1,2]. However, PVDF membranes, utilized in membrane contactor (MC) processes,have a relative weak hydrophobicityleading to undesired membrane wetting during MC processing. Due to the chemical structure of the perfluoro group, perfluoro-polymers, such as polytetrafluoroethylene (PTFE)and poly(tetrafluoroethylene-co-hexafluoropropylene) (FEP),are more hydrophobic than PVDF. Blending perfluoro-polymer with PVDF is therefore an effective way to enhance the hydrophobicity ofPVDFmembranes[3]. Teoh et al.[4] prepared PVDF/PTFE blend hollow fiber membranes by the phase inversion method. Incorporation of PTFE particles into the PVDF matrix enhanced membrane hydrophobicity, yielding a resultant water contact angle of 103° when the PTFE loading was50wt%.

Compared to other hollow fibermembranes fabrication method, melt-spinning method have the advantage that causes little to no pollution (little or no solvents) and has low costs (little or no diluents, additives) [5]. However, the obtained hollow fiber membranes have low porosity and poor permeability that limit wide application. For membranes produced by melt-spinning method, post-treatment isfrequently used to optimize performances[6-8]. Drawing and heat-treatment affect membrane morphology and performances[9-15].A great number of studies have investigated the influences of post-treatment on membrane performance.Tabatabaei et al. [16,17] studied the effects of drawing on polypropylene (PP) membrane and found that during hot drawing, the water vapor transmission rate improves with increasing the applied extension, and thatthe effect is inversed for cold drawing. Liu et al. [18]fabricatedpolyurethane-based (PU-based) hollow fiber membranes by the melt-spinning method. The influence of hot-air treatment conditions, including theoretical drawing ratio, temperature, and time, on morphology and performance of membranes were investigated.Theresultsshowthatthemaximum mean poresizeandpurewaterfluxwereobtainedatatheoreticaldrawing ratioof 2 at70°C.

In this study, PVDF/FEP blend hollow fiber membranes werefabricated using the melt-spinning method.The polymer matrix phase was composed of PVDF while the dispersed phase was composed of micro-scale FEP particles. The effects of post-treatment (drawing ratio and temperature) on the blend hollow fiber membranes' morphology werethen investigated.Finally, the performance of the PVDF/FEPblend hollow fiber membranesin vacuum membrane distillation (VMD) wasstudied.

2. Experimental

2.1 Materials

PVDF(Solef 6010, Solvay, T_m=170°C) was kindly provided bypurchased from Solvay Co., Ltd., Belgium.Micro-scale FEP particleswerepurchased fromShandong Huaxiashenzhou Co., Ltd. The solvents N,N-dimethylacetamide (DMAc) and dioctyl phthalate (DOP) (Synthesis Grade, Tianjin Kermel Chemical Reagent Co., Ltd,>99.5%,) wereused diluted without further purification.

2.2. PVDF/FEP blend hollow fiber membrane preparation and treatment

Before use, the PVDF and FEP resinswere dried for 12h at 100±2°C in a vacuum oven (-1 bar). Then, at a particular mass ratio, PVDF, FEP, DMAc and DOP were homogeneously mixed under high speed agitation. Finally, the mixture was spun into hollow fiber membranesby the melt spinning method with a twin-screw spinning machine. The spinning conditions are reported in Table 1.

Thepost-treatments of PVDF/FEP blend hollow fiber membranesare described as follows: The PVDF/FEP blend hollow fiber membranes were placed in anelectronic tensile testing machine (JBDL-200N). The blend hollow fiber membranes were stretched under a uniform speed at different drawing ratios (50, 100 and 150%)，and under various drawing temperatures (25, 50, 90, and150°C).Drawing ratio (φ) was calculated according to Eq. (1). Finally, the stretched hollow fiber membranes were fastened to maintain stretched length.

$$\varphi(\%) = \frac{L_1 - L_2}{L_2} \times 100\% \quad (1)$$

where L_2 and L_1 represent the length before and after post-treatment under tension, respectively.

Table 1 Composition and spinning parameters of melt-spun hollow fiber membranes

Table 2 Sample designations and parametersof PVDF/FEPblend membranes

2.3. Membrane characterizations

2.3.1 Morphology observations

The morphologies of surface and cross-section of prepared hollow fiber membraneswere observed using field emission scanningelectron microscopy (FESEM, X4800; Hitachi, Japan).The membraneswere immersed in liquid nitrogen for 10-15s.Then the frozen membranes were broken for cross-section observation.The specimens were fixed on the conductiveadhesive and coated with a thin layer of gold before observing[19].

2.3.2 Porosity

The membrane porosity was defined as the pore volume divided by the total volume of the porous membrane. Membrane porositywascalculated by a gravimetric method, and was calculated according to equation 2 below [20,21]:

$$\varepsilon(\%) = \frac{W_1 - W_2}{(\pi/4)(D^2 - d^2)l\sigma} \times 100\% \quad (2)$$

wherew_1 is the weight of the wet membrane (g), w_2 is the weight of the dry membrane (g), σ is then-butanoldensity (ρ=0.8098g cm^{-3}), D is the outer diameter (cm), d is the inner diameter (cm) and l is the length of sample membrane (cm).

2.3.3 Water Contact Angle

In order to evaluate the variations in the surface wetting characteristics of the PVDF/FEP blend hollow fiber membranes,the water contact angles of all the samples were measured using an optical contact angle meter (Jinshengxin Inspection instrument Co., Ltd., model JYSP-180).A water droplet was dropped on the sample surface, at least threewater contact angles at different locations wererecorded to get a reliable value,each sample was tested five times to evaluate the average value.

2.3.4 Permeability tests

The gas permeation fluxof the dry membranes was determined by equation 3.The permeate flow rate was measured under different pressures, as shown in Fig. 1. The lumen side of each membrane module was connected to a nitrogen cylinder. The permeation flux of nitrogen through the dried membranes was measured at room temperature.

$$J = \frac{L}{A} \tag{3}$$

where$J$ is the nitrogen flux ($m^3 \cdot m^{-2} \cdot h^{-1}$), L is the nitrogen flow ($m^3 \cdot h^{-1}$) and A is the membrane area (m^2).

Fig. 1 Gas permeation flux of the hollow fiber membrane testing device

The liquid entry pressure (LEP) of water was measured to evaluate the membrane wetting resistance. LEP depends on pore size and hydrophobicity of the membrane. LEP was measured using a dead-end filtration set-up, which was designed according to the method described extensively by Smolder and Franken [22]. The dry hydrophobic membrane was assessed at room temperature using a device made in the laboratory. The pressure of the feed side increased slowlyin increments of 0.01 MPa during the measurement. At each pressure interval, the membrane was kept at a constant pressure for 5 min until the first permeate drop was obtained. The corresponding pressure value was considered the LEP point. Each sample was tested three times, and the values were averaged.

2.3.5. Thermal analysis

The dynamic thermal behavior of blend membranes was determined using dynamic mechanical analysis(DMA)(DMA242C, NETZSCH, Germany) between 0-300°Cat a heating rate of 5°C·min^{-1}. The thermal properties of blend membranes were measured bydifferential scanningcalorimetry (DSC)(DSC200F3, NETZSCH, Germany). DSC was performed at a heating rate of 10°C·min^{-1} over the range of 0-300°C.

2.3.6. Membrane distillation (MD)

Vacuum membrane distillation (VMD) was conducted to evaluate the permeate performance of PVDF/FEP blend hollow fiber membranes.The water desalination experiment was performed using aset-up schematically shown in Fig. 2.The shell side of the membrane was in contact with ahot, circulatingNaClaqueous solution (3.5wt%) while its lumen side was connected to a vacuumpump to withdraw the permeated water vapor.The water vapor was subsequently condensed by a glass condenser using tap water as coolant. The condensed waterwas collected in a glass bottle, and its volume was determined with ameasuring cylinder. The conductivity of the feed solution and permeatewater were measured by a conductivity meter (AP-2, HM). The NaCl rejectionR was calculated by equation 4.

$$R = \left(1 - \frac{C_P}{C_f}\right) \times 100\% \quad (4)$$

whereC_f and $C_p$were the conductivities of the feed solution and permeatewater, respectively.

Fig.2 Schematic of vacuum membrane distillation (VMD) system

(1-water bath; 2-magnetic circulating pump; 3-meter; 4-pressure gauge; 5-valve;6-membrane component; 7-condenser pipe; 8-water flask; 9-vacuum pump)

3. Result and discussion

3.1 Membranes stress-strain curves

Effects of drawing temperature on the stress-strain curves of PVDF/FEP blend hollow fiber membranes are shown in Fig. 3. All the curves displayed a typical yield when the drawing ratio was 20~30%. While asthe drawing temperature increased, the yield stress values reduced, and the yield point gradually weakened and eventually disappeared. With the increase indrawing temperature, polymer macromolecules have more movement,and therefore, the forces between molecules decrease.When the drawing temperature was lowered, the intermolecular forcebecame larger, and the initial modulus of the PVDF/FEP blend hollow fiber membranebecamehigher.Meanwhile, the blend membranes' breaking strength and

initial modulus increased monotonicallywith the decrease indrawingtemperature.This may be due to the higher drawing temperature inducinga higherpolymer chain activity, which resulted in a greater orientation of the hollow fiber membrane under the same stress.

Fig. 3 Stress-strain curves of PVDF-FEP blend hollow fiber membranes. Drawing ratio: (a) 50%; (b) 100%; (c) 150%

3.2 Formation mechanism of IFMs

Regarding the method to produce polymeric hollow fiber membranes, pore formation of themelt spinning method was much more difficultthan solution spinning. Therefore, it was essential to improve the permeability of melt spun hollow fiber membranes. In our previous studies[18,23,24], nano-scale inorganic particles were introduced into the membrane polymer to create the IFMs by drawing. During the drawing process, IFMs formed between the polymer matrix and the dispersed phase of the inorganic particles. IFMs improved the porosity and permeability of hollow fiber membraneswithout reducing mechanical strength. In this study, the polymer particle of FEP was the dispersed phase,responsible for the strong hydrophilicity and the same C-F structure with PVDF. The formation mechanism of IFMs is shown in Fig. 4. Nascent PVDF/FEP hollow fiber membranes were composed of a continuous phase (PVDF) and a dispersed phase (FEP). To the best of our knowledge, the FEP particles kept asphericalshape. FEPhad good rigidity under the spinning temperature of 170°C, while the PVDF melted into fluid wrapping the FEP particles. When the blend hollow fiber membraneswere drawn, there was an interface between the continuous phase and the dispersed phase due to separation. Furthermore, there were crazes in PVDFindicating damage to the amorphous regions during the drawing process.

Fig. 4 The mechanism of IFM formation within drawn PVDF/FEP blend membranes

3.3Dynamic Mechanical Analysis

DMA curves of stretched PVDF/FEP blend hollow fiber membranesare shown in Fig. 5.The highest storage modulus (E')was at a drawing ratio of 100% under the same drawing temperature (90°C). When the drawing ratio washighenough (150%), an excess orientation was induced.The molecular arrangement had an excess orderliness, and the molecular interaction was too large. The elasticity of the blend hollow fiber membrane deteriorated. At the same drawing ratio, the storage modulus increased with the increase indrawingtemperature. With increasing temperature, the material was more easily deformed.Along the direction of the stress, the polymer structure was in a more orderly arrangement, and there was anincreasein the degree of crystallinity.Duringthe drawing process, the ordered structure resulted in a larger rebound force, which wascharacterized by better elasticity.

As shown in Fig. 5(b), DMA was used to observe the relationship between Tanδ and temperature. Tanδof a polymer is an important criterion for the compatibility of components[25,26]. The Tanδvalue of PVDF wasabout 170°C,and that of FEP wasabout 275°C. Analysis ofPVDF/FEP blend hollow fiber membranes showedapeak near 180-200°C and another near250 °C. These peaks corresponded to thePVDF Tanδpeak and the FEP Tanδpeak, respectively.When compared to the peaks of the two pure polymers, the Tanδpeak of PVDF in the blendmoved to the rightof that of the pure polymer, while the blend peak of FEP moved to the left of that of the pure polymer. The two Tanδpeaks were close to each other, which indicated thatPVDF and FEP werepartially compatible in thermodynamics.

Fig.5 DMA thermograms of post-treatedPVDF/FEP blend hollow fiber membranes

(a) E' versus temperature; (b) Tanδ versus temperature

3.4Differential Scanning Calorimetry

DSC curves of the post-treated PVDF/FEP blend hollow fiber membranes under different drawing conditions are presented in Fig. 6. The melting peaks of the stretched PVDF/FEP blend hollow fiber membranes occurred around 172°C and 260°C corresponding to PVDF and FEP, respectively. This indicated that PVDF and FEP

werephysically mixed.The addition ofFEP did not change the crystal structure of PVDF, and thiswas consistent with the DMAresults.As shown in Fig.6(a), the peak width of PVDF became widerat first and then became narrower.The peak area of PVDFat first decreased but then increased with increasingdrawing ratios becausethe unstable crystalline phases were destroyed during the drawing process.With further drawing, the macromolecular chain orientation became regular, and this induced the improvement of the crystallinity.As can be seen from Fig. 6(b), under the same drawing ratio, there wereno changes in thePVDF melting peak area,andthe peak width became narrower with increasingdrawing temperature. This might be becausethe macromolecular chains moved easierand arrangedmore regularly with an increase indrawing temperature.Also, some thin lamellae crystals were destroyed to form some thicker lamellae crystalswhichwould have made crystallization more perfect.

Fig. 6DSC thermogramsof post-treatedPVDF/FEP blend hollow fiber membranes

(a) Varying drawing ratio; (b) Varying drawingtemperature

3.5 Effect of the post-treatment on membrane's permeability

The permeability of PVDF/FEP blend hollow fiber membranes was characterized in terms of N_2 flux as shown in Fig. 7. The N_2 flux increased with an increasingdrawing ratio. Increasing the drawing ratio resulted in higher porosity and IFMs' size, which further induced higher N_2 flux. With regards todrawing temperature, the N_2 flux first increased and then decreased as the drawing temperature increased at the same drawing ratio. The first increase of the N_2 fluxis explained by the same reason of the improvement of membrane porosity and IFMs' size when the drawing temperature was lower than 50°C. To understand the decrease in the N_2 flux, the glass transition temperature (Tg) of the FEP dispersed phase wasapproximately 90-95°C. Therefore, as the drawing temperature rose to 90°C,FEP polymer macromolecular chains also began to move, and FEP particles became deformed under tensile stress-elongation refinement. Some IFMs deformed into a long-narrow shape, and some even closed, inducing the decrease in pore size.In conclusion, the pure water flux (PWF)of

PVDF/FEP blend hollow fiber membranesfirst increasedand then decreased with increasing temperature.

The trends of PVDF/FEP blend hollow fiber membranes' porosity by different post-treatments is shown in Fig.8. The porosity of theP0 membrane was low. The porosity at first only slightly increased, and then significantly increased with an increase indrawing ratio. When the drawing ratiowas low, increasing the temperature did not improve the porosity of the PVDF/FEP blend hollowfiber membranes. At low drawing ratios andincreasingdrawing temperature (above the Tgof FEP particles), both PVDF and FEP polymers deformed, the interface microvoids reduced, and porosity decreased. At largedrawing ratios, the porosity of PVDF/FEP blend hollow fiber membranes significantly improved. Porosity increased because the tensile stresscaused more IFMs inthe blend hollow fiber membranes,and the tensile stress widenedthe original micropores.Under same drawing ratio, the porosity first decreased and then increased with increasingdrawing temperature. The results agreed well with the permeability results as discussed above.

The effects of post-treatment on the LEP of PVDF/FEP blend hollow fiber membranes are illustrated in Fig. 9. For the hydrophobic membrane, the pore size and hydrophobicity dramatically affected the value of LEP. As shown in Fig. 9, with an increase in the drawing ratio, the LEP of PVDF/FEP blend hollow fiber membrane decreased and was more than 0.4MPa.The decrease of LEP attributed to the size enhancement of IFMs, and this agreed very well with the analysis above.

Fig.7 Effect of the post-treatment on N_2 flux

Fig.8 Effect of the post-treatment on porosity

Fig.9 Effect of the post-treatment on LEP

In Fig. 10, the changes in the water contact angles of the post-treated PVDF/FEP blend hollow fiber membranes are displayed. The static contact angle of the P0

membrane was 116.3° .With an increase in the drawing ratio, more IFMs were produced in the PVDF/FEP blend hollow fiber membrane's surface, and therefore, the water was more likely to wet the surface of PVDF/FEP blend hollow fiber membrane as the static contact angle decreased.

Fig. 10 Effect of the post-treatment on the water contact angle

3.6Effects of the post-treatment on membrane morphology

The outer surface morphologies of the post-treated PVDF/FEP blend hollow fiber membranes are shown in Fig. 11. The outer surface of the PVDF/FEP blend hollow fiber membrane P0,preparedby melt spinning method, was relatively dense.However, the outer surface was uneven fromtheFEP particles that weretrappedwithin thePVDF polymer.After post-treatment, the outer surface of the PVDF/FEP blend hollow fiber membrane changed significantly. The outer surface's pores of the blend membrane became larger with increasingdrawing ratio becausePVDF and FEP were partially compatible.PVDF/FEP blend hada stress concentration regionduring the process of drawing.As well, the outer surface may have some defects,and when tensile stress was applied tothe defects, irregular, elongatedpores appearedatthe surfacealong the drawing direction.The inner surface morphologies of the post-treated PVDF/FEP blend hollow fiber membranes are shown in Fig. 12.There were significant differences in morphology between the inner and the outer surfaces. The inner surface exhibited a much higher porosity than the outer surface. The porosity of the inner surface of the P0 membrane was less than that of the blend membrane. With an increase in the drawing ratio, the number of pores increasedin the inner surface, and the pore sizes of post-treated blend membrane became larger.IFMswere clearly observedin the inner surface.When the temperature reachedthe Tgof FEP particles, the IFMs became more narrow and evenpartiallyclosed when drawing ratioincreased.

Fig.11 Effect of post-treatment on the outer surface morphology of PVDF/FEP blend membrane(drawing temperature: A-25℃, B-50℃, C-90℃, D-130℃,drawing ratio:1-50%, 2-100%, 3-150%)

Fig.12 Effect of post-treatment on the inner surface morphology of PVDF/FEP blend membrane (drawing temperature: A-25℃, B-50℃, C-90℃, D-130℃, drawing ratio:1-50%, 2-100%, 3-150%)

The cross-section morphologies of the post-treated PVDF/FEP blend hollow fiber membranes areshown in Fig. 13.A large number of FEP particles were dispersed in the polymer membrane.The P0 membrane's cross-section was dense and exhibited a muchlower porosity. With an increase in the drawing ratio, the number of pores increasedwhile the pore sizes became larger.

Fig.13 Effect of post-treatment on the cross-section morphology of PVDF/FEP blend membrane (drawing temperature: A-25℃, B-50℃, C-90℃, D-130℃, drawing ratio:1-50%, 2-100%, 3-150%)

3.7 Membrane distillation performance

The post-treatedPVDF/FEP blend hollow fiber membranes were tested for the VMD process,and permeate flux results are shown in Fig. 14. The maximum permeate flux of the N15 membrane reached as highas 3.2 $L \cdot m^{-2} \cdot h^{-1}$. Moreover, with an increasing drawing ratio, permeate fluxincreased due to the increased number and pore sizes of IFMs. Thus, membrane distillation (MD) flux had an obvious growth trend as thedrawing ratioincreased.

Fig. 14 Influence of post-treatment on the PVDF/FEP blend hollow fiber membrane distillation flux, 1-Raw, 2-N5, 3-N10, 4-N15

The salt rejection of apost-treated PVDF/FEP blend hollow fiber membrane module at an operating temperature of 70°Cis shown in Fig. 15.All PVDF/FEP blend hollow

fiber membrane desalination rateswere higher than 99% among thedifferent post-treatment conditions. The P0 membrane desalination rate was significantly higher than that of post-treatedPVDF/FEP blend hollow fiber membrane, and the desalination rateswere relatively stable.

Fig. 15 The effect of post-treatment on the PVDF/FEP blend hollow fiber membrane component of desalting

4. Conclusions

PVDF/FEP blend hollow fiber membranes were fabricated by the melt-spinning method. Effects of drawing ratio and temperature on the structure and the performances of PVDF/FEP blend hollow fiber membranes were investigated. Increasing thedrawing ratio induced an increase in both the pore number and size of theouter surface. The porosity and PWF of the PVDF/FEP blend membrane was significantly promoted while the LEP decreased as the drawing ratioincreased.It was concluded that the PVDF and FEP were partially compatible systems from the results of DSC and DMA analysis.

Acknowledgments This work was supported by National Natural Science Foundation of China (No.21404079, 51402212), Tianjin Key Research Program of Application Foundation and Advanced Technology (No.12JCZDJC26600).

References

[1] J.E. Dohany, L.E. Robb, Polyvinylidene fluoride, 3rd, Kirk-Othmer Encyclopedia ofChemical Technology, 11, Wiley, New York, 1980, p. 64.

[2] A.J. Lovinger, Poly(vinylidene fluoride), in: D.C. Bassett (Ed.), Development inCrystalline Polymers, Appl. Sci, 1(1982) p. 195.

[3] Guo-dong Kang, Yi-mingCao, Application and modification of poly(vinylidene fluoride) (PVDF) membranes, J. Membr. Sci.463 (2014) 145-165.

[4] M.M. Teoh,T.S.Chung,Membranedistillationwithhydrophobicmacrovoid-free PVDF-PTFE hollow fiber membranes,Sep.Purif.Technol.66(2009) 229-236.

[5] J. Kim, S.S. Kim, M. Park, M. Jang, Effects of precursor properties on the preparation of polyethylene hollow fiber membranes by stretching, J. Membr. Sci. 318 (2008) 201-209.

[6] Lee J, Lee H K, Rasmussen K E, et al. Environmental and bioanalytical applications of hollow fiber membrane liquid-phase microextraction: a review,Analyticachimicaacta. 624(2008) 253-268.

[7] Song K, Zhang Y, Meng J, et al. Structural polymer-based carbon nanotube composite fibers: understanding the processing–structure–performance relationship, Materials. 6(2013) 2543-2577.

[8] Zhao C, Zhou X, Yue Y. Determination of pore size and pore size distribution on the surface of hollow-fiber filtration membranes: a review of methods, Desalination., 129(2000) 107-123.

[9] I.C. Kim, H.G. Yun, K.H. Lee, Preparation of asymmetric polyacrylonitrile membrane with small pore size by phase inversion and post-treatment process, J. Membr. Sci. 199 (2002) 75-84.

[10] L.S. Wan, Z.K. Xu, X.J. Huang, A.F. Che, Z.G. Wang, A novel process for the post-treatment of polyacrylonitrile-based membranes: performance improvement and possible mechanism, J. Membr. Sci. 277 (2006) 157-164.

[11] S.H. Tabatabaei, P.J. Carreau, A. Ajji, Microporous membranes obtained from polypropylene blend films by stretching, J. Membr. Sci. 325 (2008) 772-782.

[12] M.T. Liu, C.F. Xiao, X.Y. Hu, Optimization of polyurethane-based hollow fiber membranes morphology and performance by post-treatment methods, Desalination 275 (2011) 133-140.

[13] H.L. Liu, C.F. Xiao, X.Y. Hu,M.T. Liu,Post-treatment effect on morphology and performance of polyurethane-based hollow fiber membranes through melt-spinning method, J. Membr. Sci. 427 (2013) 326-335.

[14] J.J. Kim, T.S. Jang, Y.D. Kwon, U.Y. Kim, S.S. Kim, Structural study of microporouspolypropylene hollow fiber membranes made by the melt-spinning and coldstretchingmethod, J. Membr. Sci. 93 (1994) 209-215.

[15] S.Y. Lee, S.Y. Park, H.S. Song, Lamellar crystalline structure of hard elasticHDPE films and its influence on microporous membrane formation, Poly. 47 (2006) 3540-3547.

[16] S.H. Tabatabaei, P.J. Carreau, Abdellah.Ajji, Microporous membranes obtained from polypropylene blend films by stretching, J. Membr. Sci. 325 (2008) 772-782.

[17] A. Rahimpour, et al., The effect of heat treatment of PES and PVDF ultrafiltrationmembranes on morphology and performance for milk filtration, J. Membr. Sci. 330 (2009) 189-204.

[18] Hailiang Liu,ChangfaXiao, XiaoyuHu,MeitianLiu, Post-treatment effect on morphology and performance of polyurethane-based hollow fiber membranes through melt-spinning method, J. Membr. Sci.. 427 (2013) 326-335.

[19] H.A. Tsai, et al., Heat-treatment effect on the morphology and pervaporationperformances of asymmetric PAN hollow fiber membranes, J. Membr. Sci. 255 (1-2) (2005) 33-47.

[20] L.F.Han,Z.L.Xu,Y.Cao,Y.M.Wei,H.T.Xu,Preparation,characterizationand permeation propertyofAl_2O_3, Al_2O_3-SiO_2 and Al_2O_3-kaolin hollowfiber membranes, J.Membr.Sci.372(2011)154-164.

[21] X.F.Li,Y.G.Wang,X.L.Lu,C.F.Xiao,Morphologychangesofpolyvinylidene fluoride membraneunderdifferentphaseseparationmechanisms,J.Membr. Sci. 320(2008) 477-482.

[22] K. Smolders, A.C.M. Franken, Terminology for membrane distillation, Desalination.72 (1989) 249-262.

[23] Qinglin Huang, Changfa Xiao,Xiaoyu Hu and Shulin An, Fabrication and properties of poly(tetrafluoroethylene-cohexafluoropropylene)hollow fiber membranes, J. Mater. Chem. 21(2011) 16510-16516

[24] Meitian Liu, Changfa Xiao, Xiaoyu Hu, Optimization of polyurethane-based hollow fiber membranes morphology andperformance by post-treatment methods, Desalination.275 (2011) 133-140.

[25] Zeng S, Reyes C, Liu J, et al. Facile hydroxylation of halloysite nanotubes for epoxy nanocomposite applications, Poly. 55(2014)6519-6528.

[26] Song K, Zhang Y, Minus M L. Polymer Interphase Self−Reinforcement and Strengthening Mechanisms in Low−Loaded Nanocomposite Fibers, Macromolecular Chemistry and Physics, 216 (2015) 1313-1320.

Appendices

Eq (1): $$\varphi(\%) = \frac{L_1 - L_2}{L_2} \times 100\%$$

Eq(2): $$\varepsilon(\%) = \frac{W_1 - W_2}{(\pi/4)(D^2 - d^2)l\sigma} \times 100\%$$

Eq(3): $$J = \frac{L}{A}$$

Eq(4): $$R = \left(1 - \frac{C_P}{C_f}\right) \times 100\%$$

List of symbols

Symbol	Defination	Unit
φ	Drawing ratio	%
L	Length of membrane	m
ε	Porosity	%
W	Weight of membrane	g
D	outer diameter	cm
d	inner diameter	cm
J	Nitrogen flux	$m^3 \cdot m^{-2} \cdot h^{-1}$
R	NaCl rejection	%
C_p	conductivities of the feed solution	μs/cm
C_f	conductivities of the permeatewater	μs/cm

Table and Figurelegends

Table:

Table 1 Composition and spinning parameters of melt-spun hollow fiber membranes

Table2 Sample designations and corresponding post-treatment parametersof evaluated PVDF/FEP blend hollow fiber membranes

Figure:

Fig.1 Gas permeation flux of the hollow fiber membrane testing device

Fig.2 Schematic of vacuum membrane distillation (VMD) system

Fig.3 Stress-strain curves of PVDF-FEP blend hollow fiber membranes. Drawing ratio: (a) 50%; (b) 100%; (c) 150%

Fig.4 The mechanism of IFM formation within drawn PVDF/FEP blend membranes

Fig.5 DMA thermograms of post-treated PVDF/FEP blend hollow fiber membranes (a) E' versus temperature; (b) Tanδ versus temperature

Fig.6 DSC thermogramsof post-treatedPVDF/FEP blend hollow fiber membranes (a) Varying drawing ratio; (b) Varying drawing temperature

Fig.7 Effect of the post-treatment on N_2 flux

Fig.8 Effect of the post-treatment on porosity

Fig.9 Effect of the post-treatment on LEP

Fig.10 Effect of the post-treatment on the water contact angle

Fig.11 Effect of post-treatment on the outer surface morphology of PVDF/FEP blend membrane(drawing temperature: A-25℃, B-50℃, C-90℃, D-130℃, drawing ratio:1-50%, 2-100%, 3-150%)

Fig.12 Effect of post-treatment on the inner surface morphology of PVDF/FEP blend membrane(drawing temperature: A-25℃, B-50℃, C-90℃, D-130℃, drawing ratio:1-50%, 2-100%, 3-150%)

Fig.13 Effect of post-treatment on the cross-section morphology of PVDF/FEP blend membrane(drawing temperature: A-25℃, B-50℃, C-90℃, D-130℃, drawing ratio:1-50%, 2-100%, 3-150%)

Fig.14 Influence of post-treatment on the PVDF/FEP blend hollow fiber membrane distillation flux, 1-Raw, 2-N5, 3-N10, 4-N15

Fig. 15 The effect of post-treatment on the PVDF/FEP blend hollow fiber membrane component of desalting

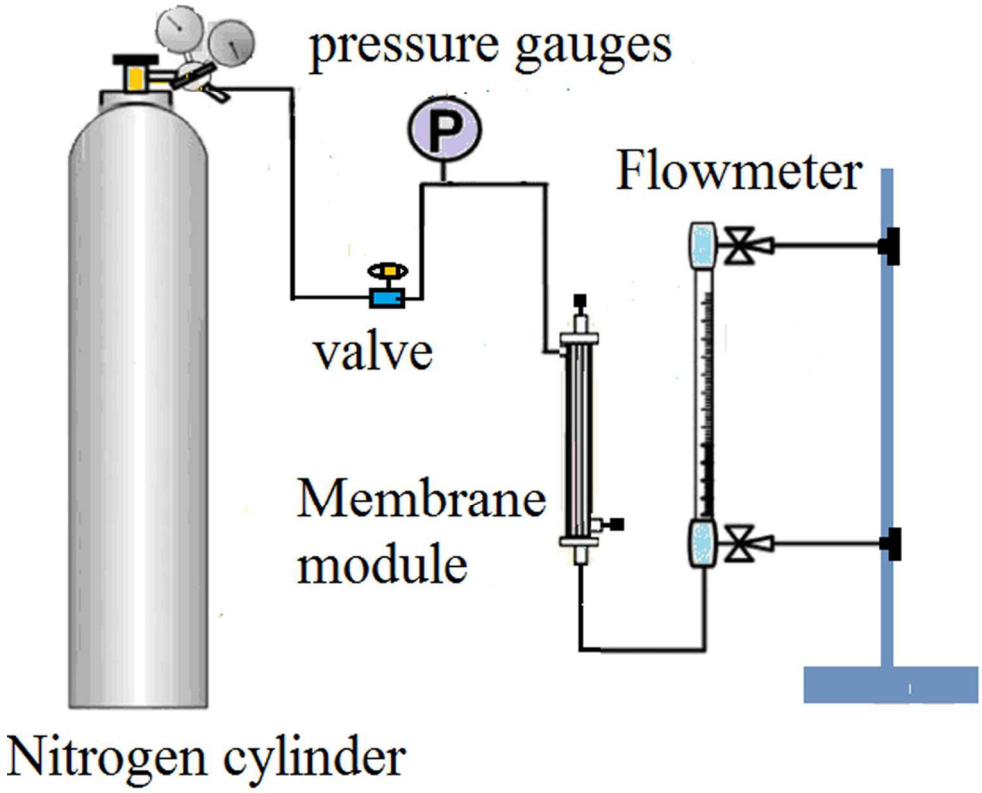

104x86mm (300 x 300 DPI)

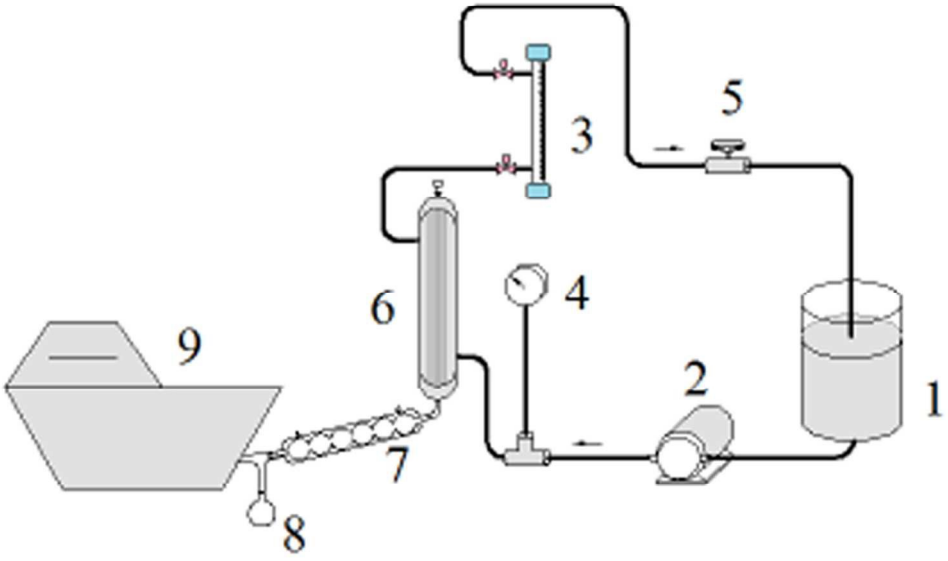

85x56mm (300 x 300 DPI)

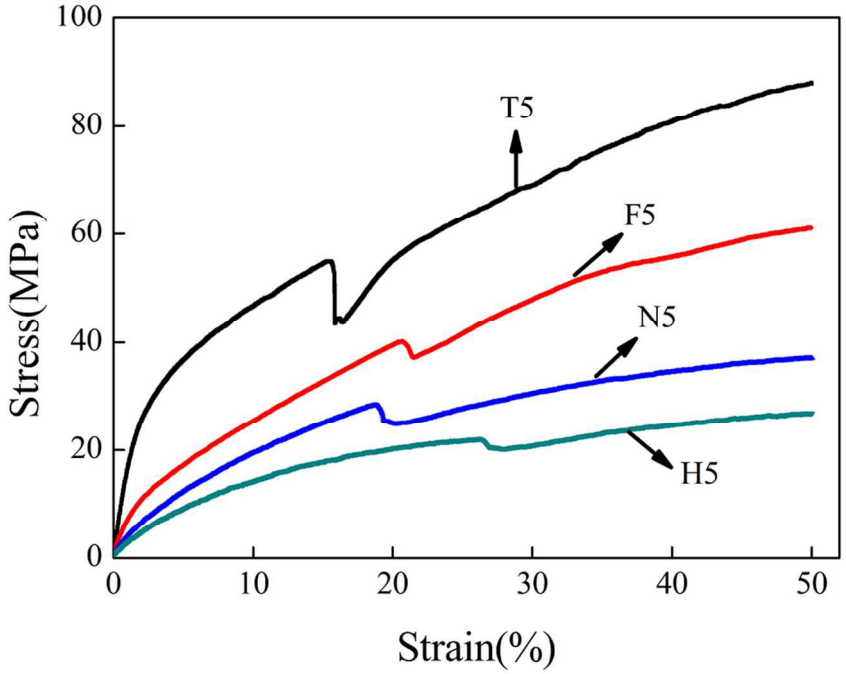

103x84mm (300 x 300 DPI)

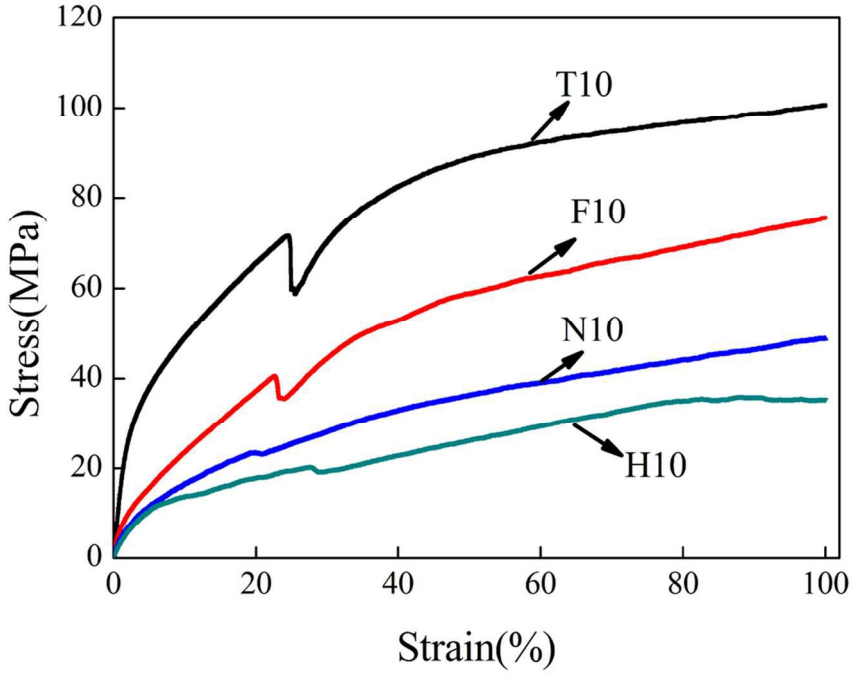

103x84mm (300 x 300 DPI)

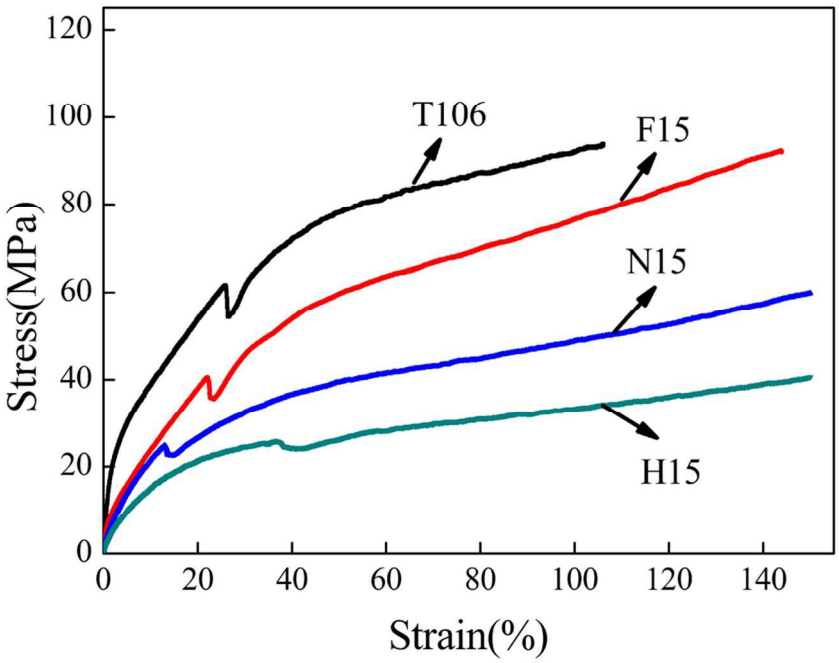

Fig.3(c)
103x83mm (300 x 300 DPI)

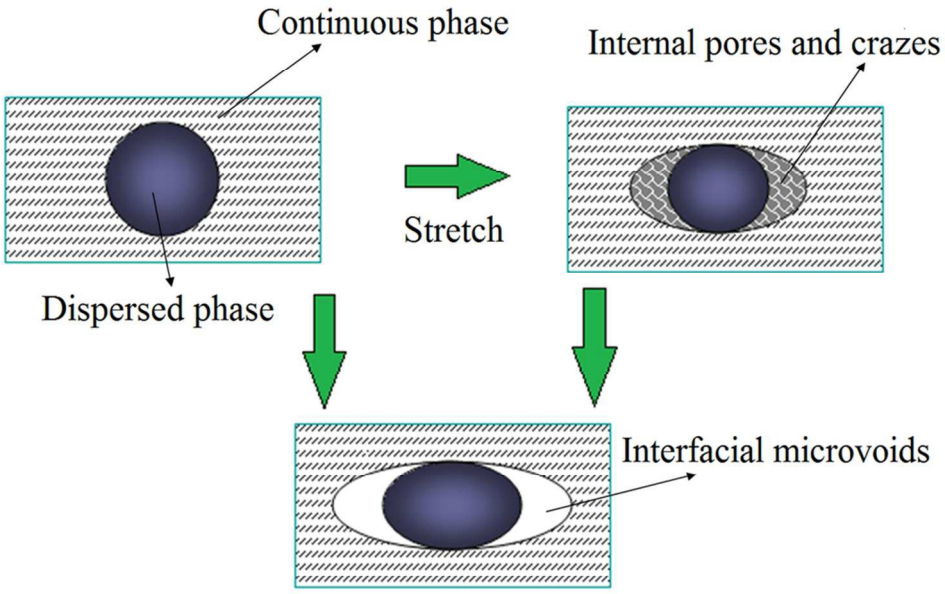

Fig.4
89x63mm (300 x 300 DPI)

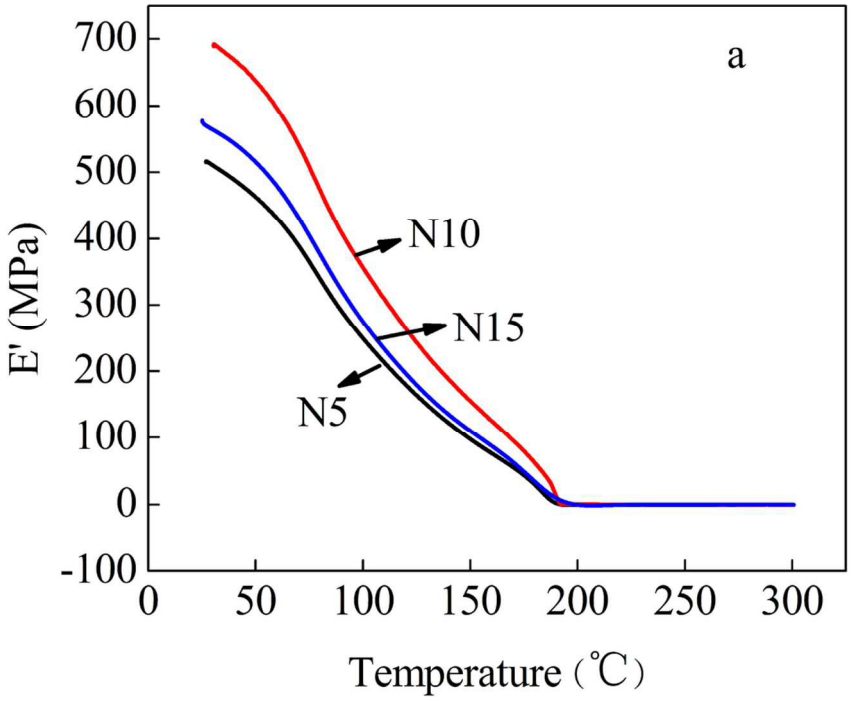

Fig.5(a)a
107x91mm (300 x 300 DPI)

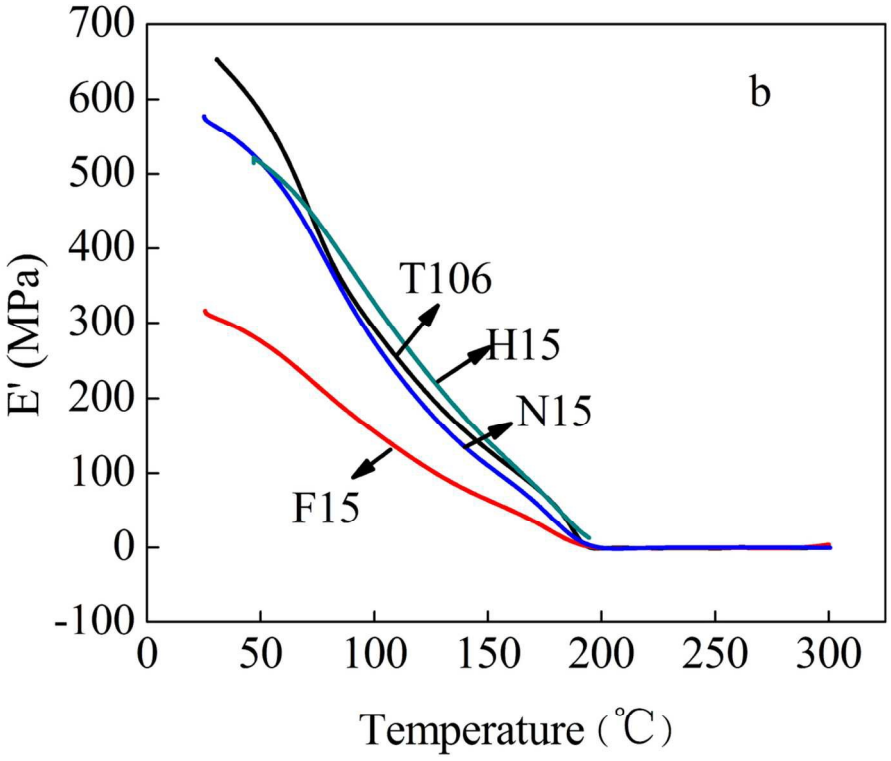

Fig.5(a)b
111x97mm (300 x 300 DPI)

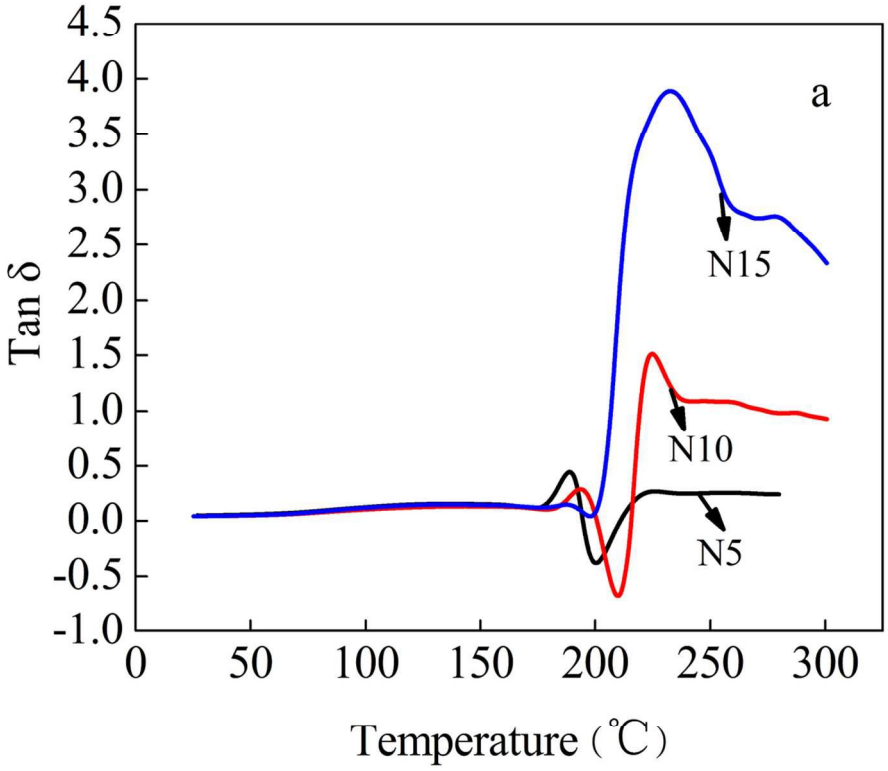

Fig.5(b)a
112x100mm (300 x 300 DPI)

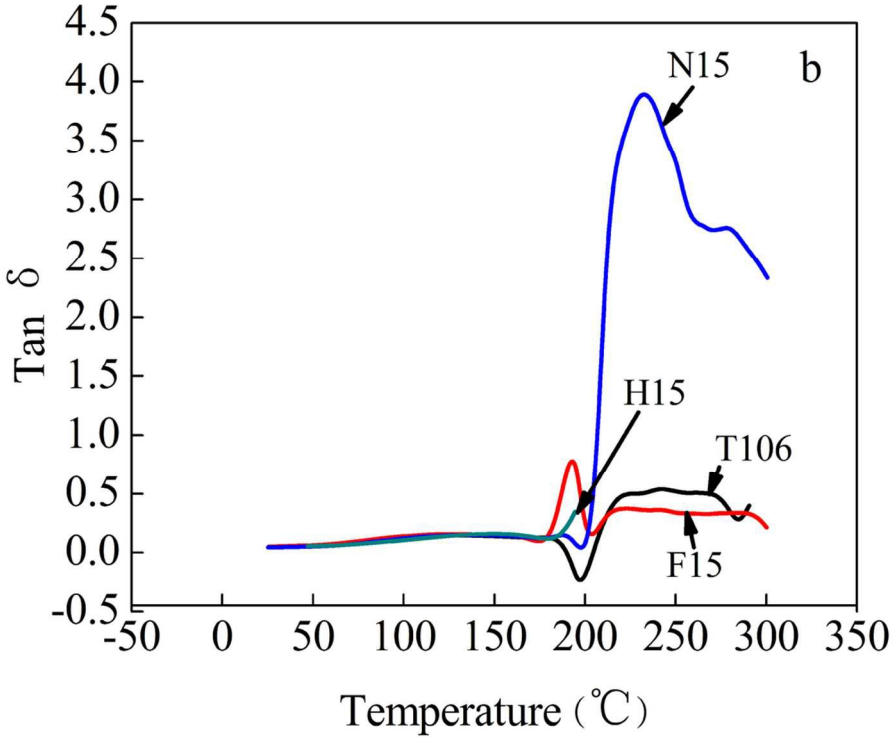

Fig.5(b)b
108x92mm (300 x 300 DPI)

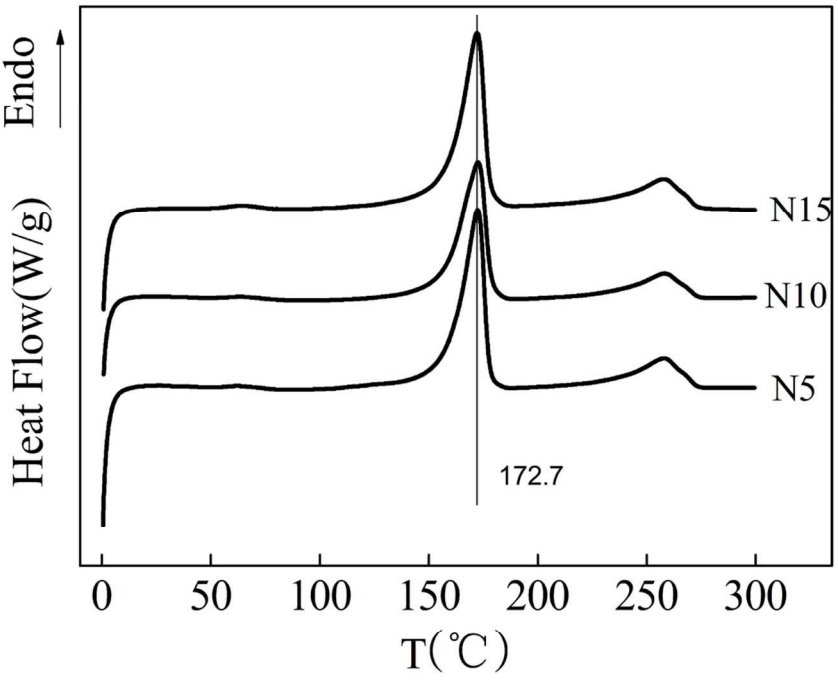

106x89mm (300 x 300 DPI)

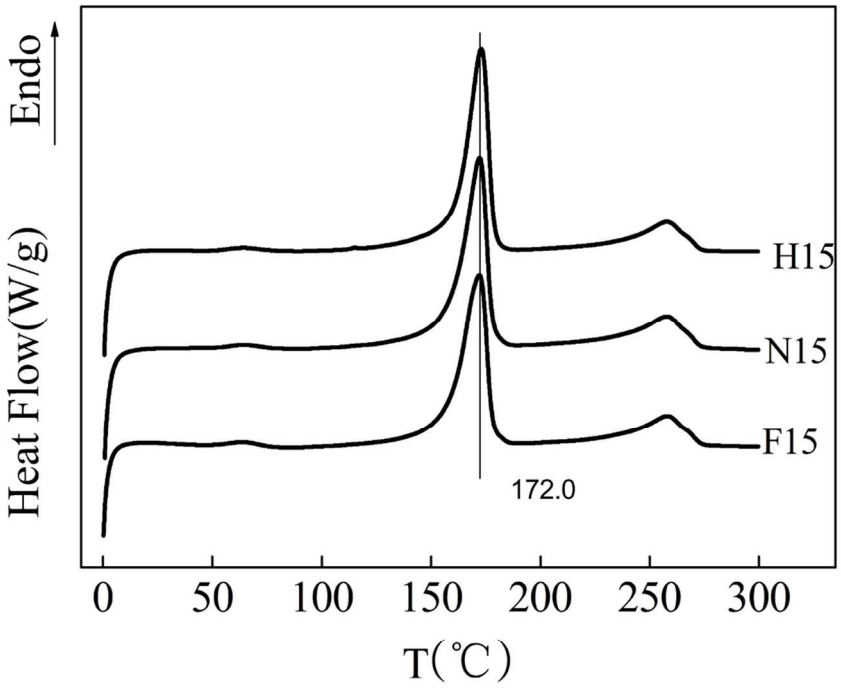

107x91mm (300 x 300 DPI)

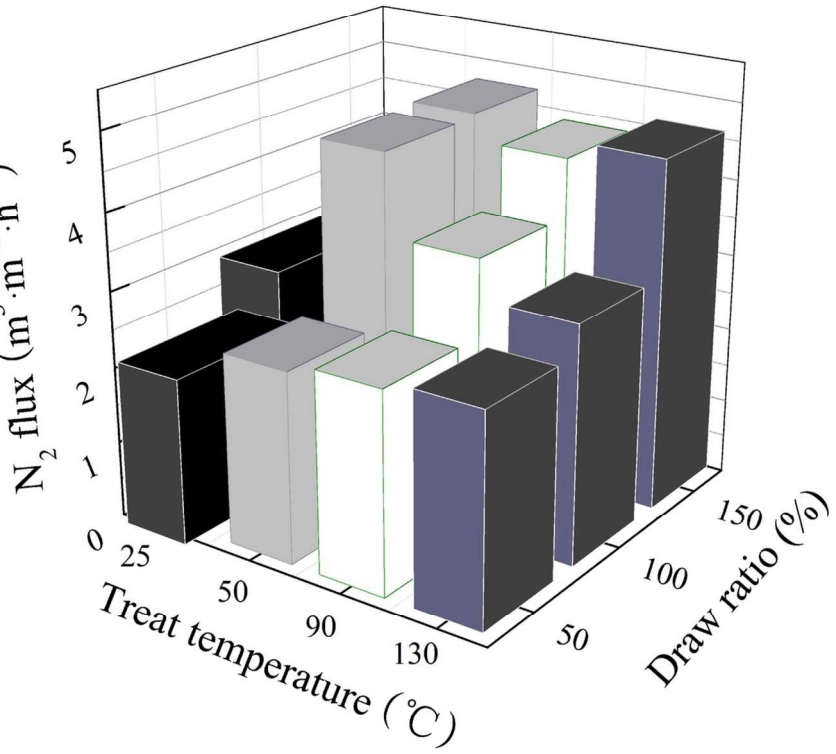

114x102mm (300 x 300 DPI)

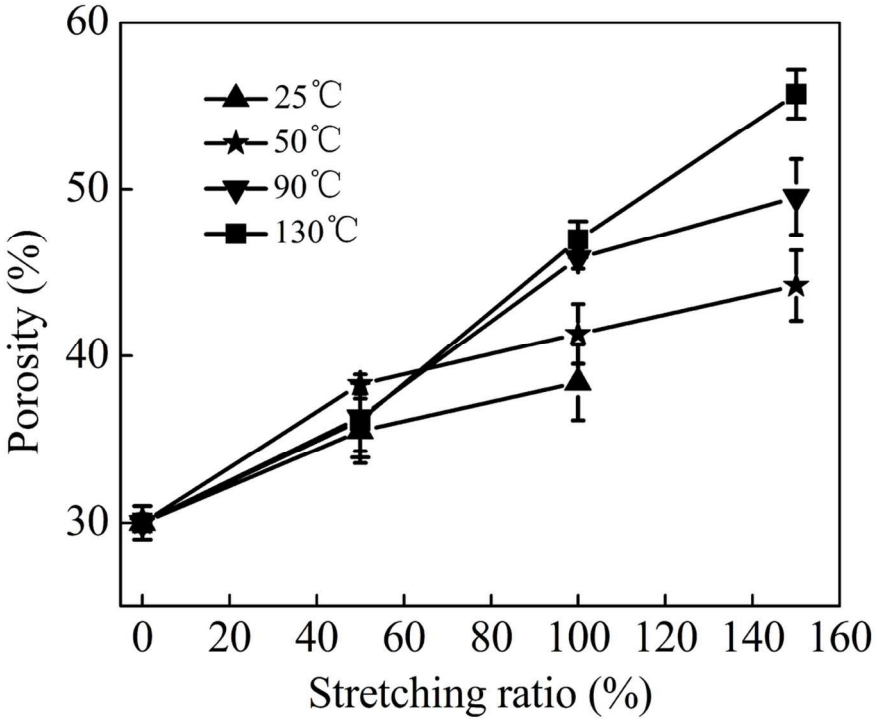

108x93mm (300 x 300 DPI)

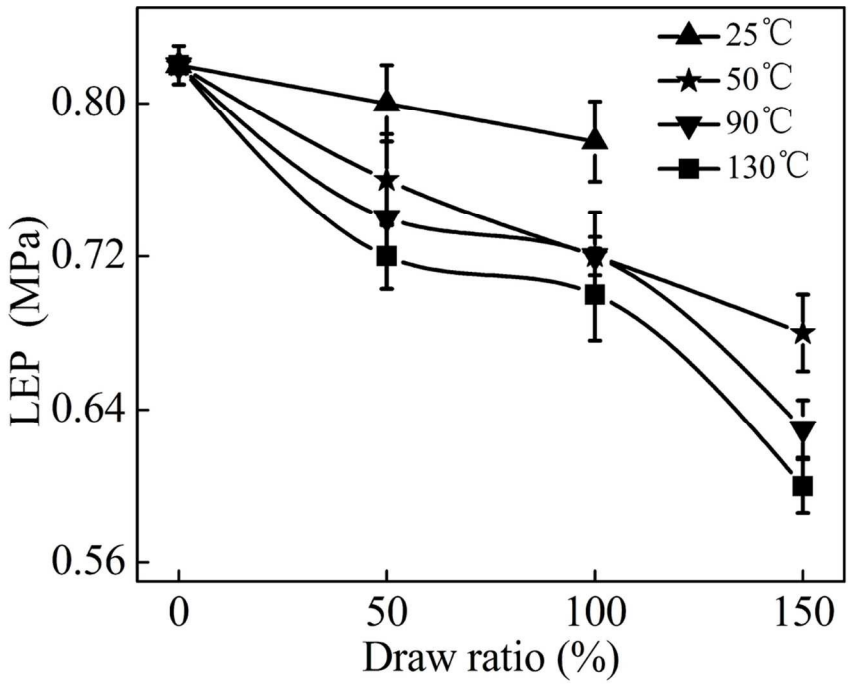

105x88mm (300 x 300 DPI)

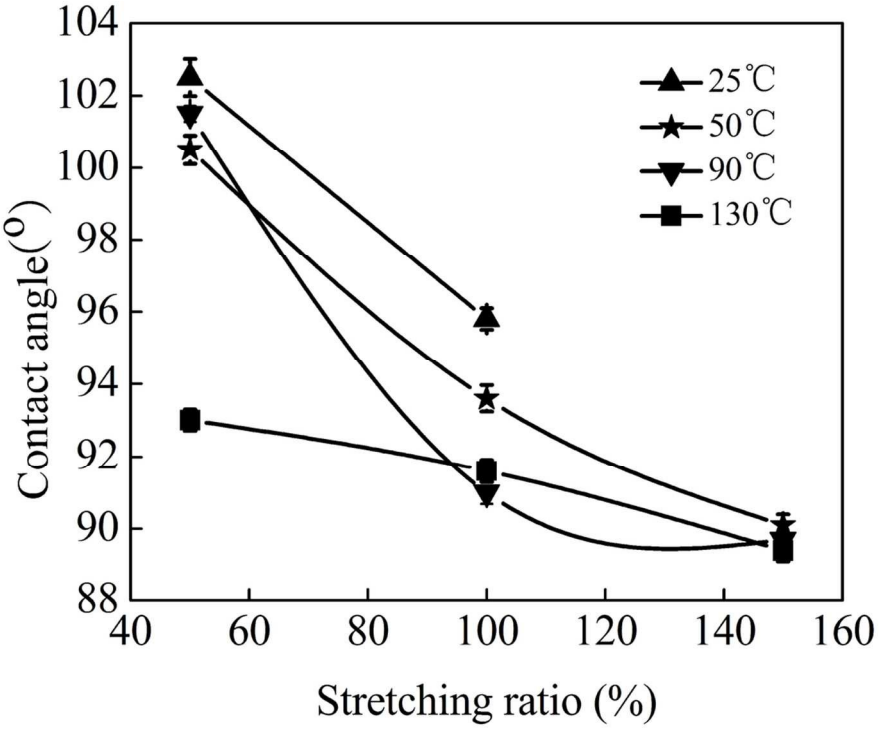

106x89mm (300 x 300 DPI)

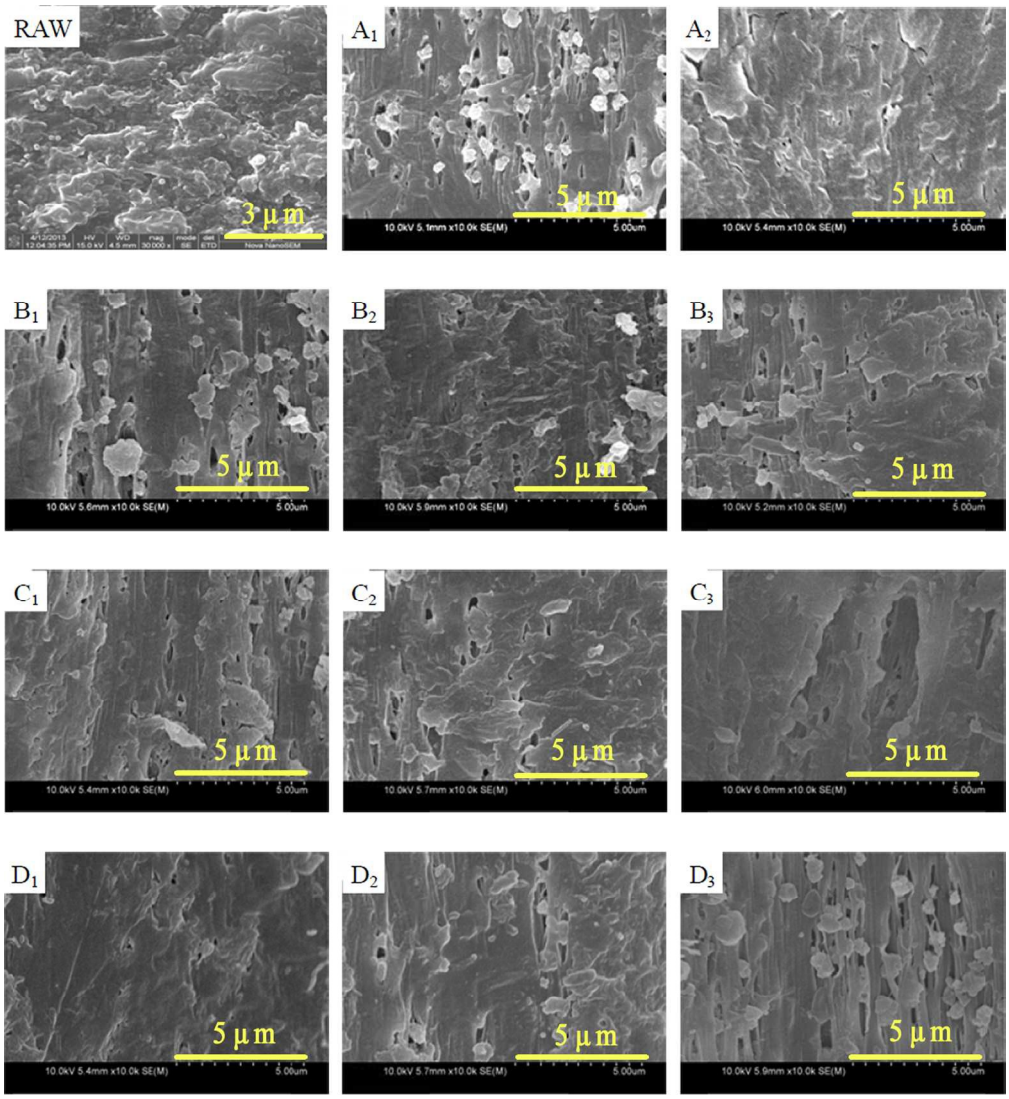

127x138mm (300 x 300 DPI)

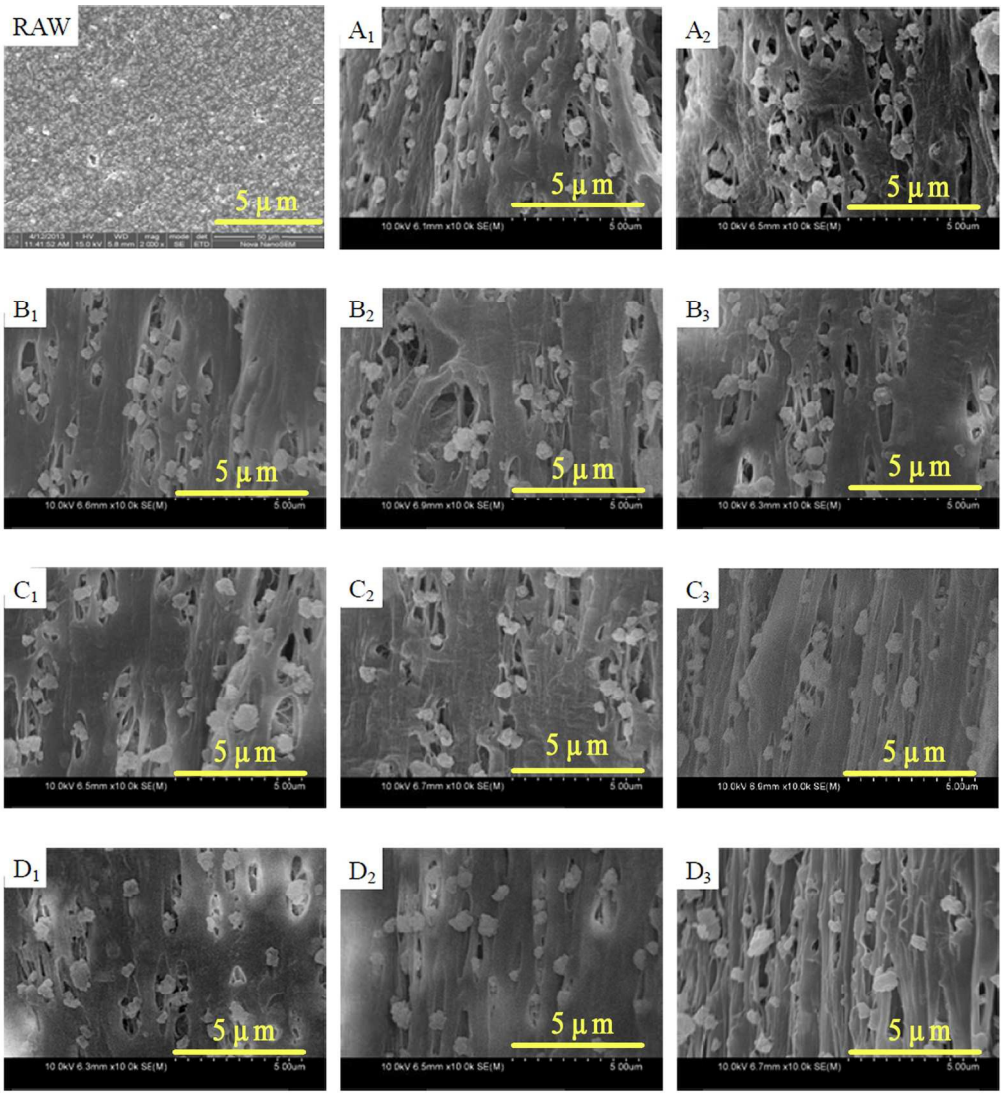

127x138mm (300 x 300 DPI)

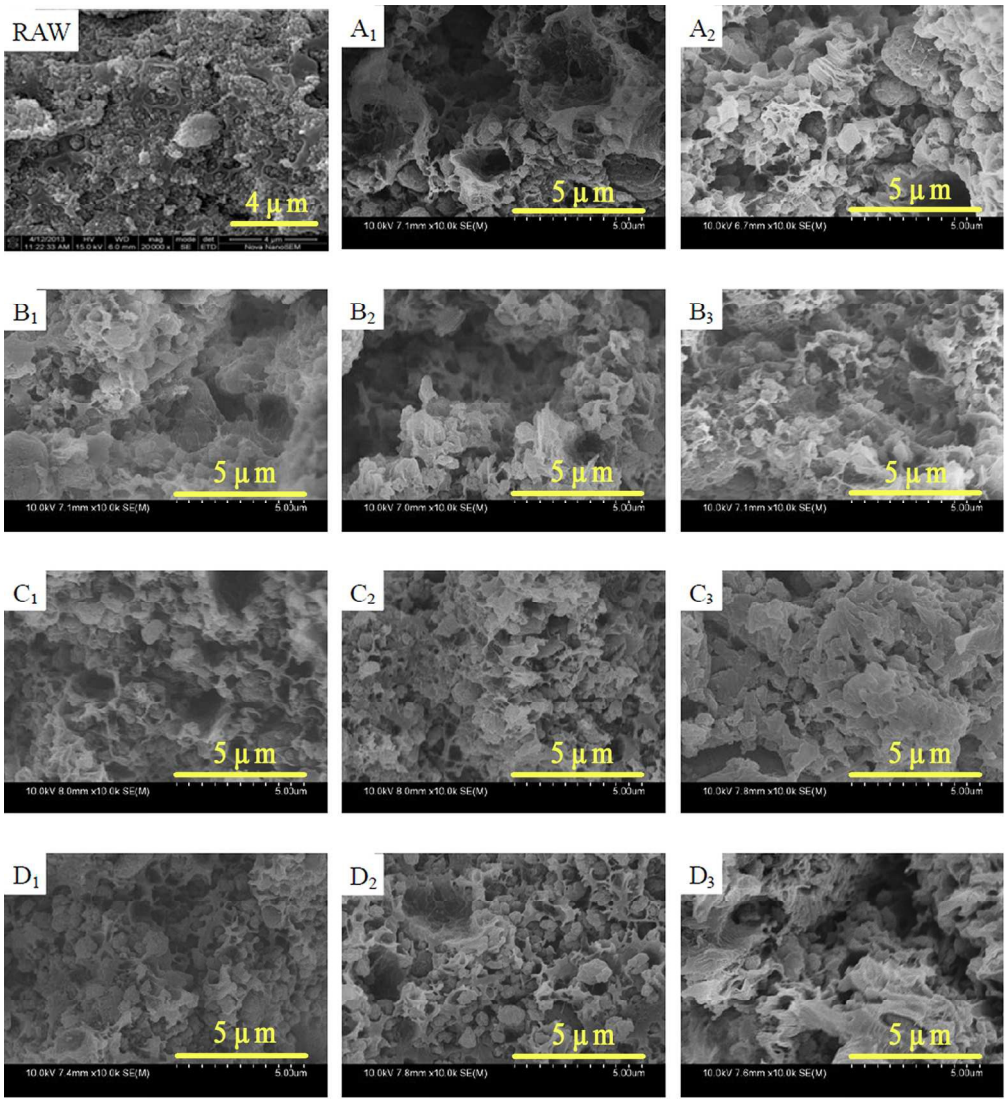

127x138mm (300 x 300 DPI)

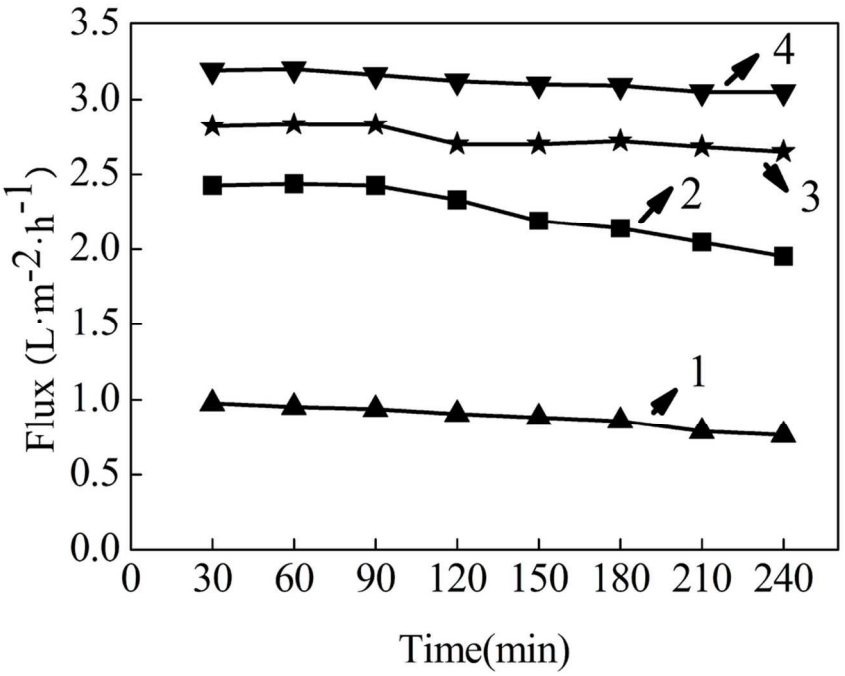

Fig.14
102x82mm (300 x 300 DPI)

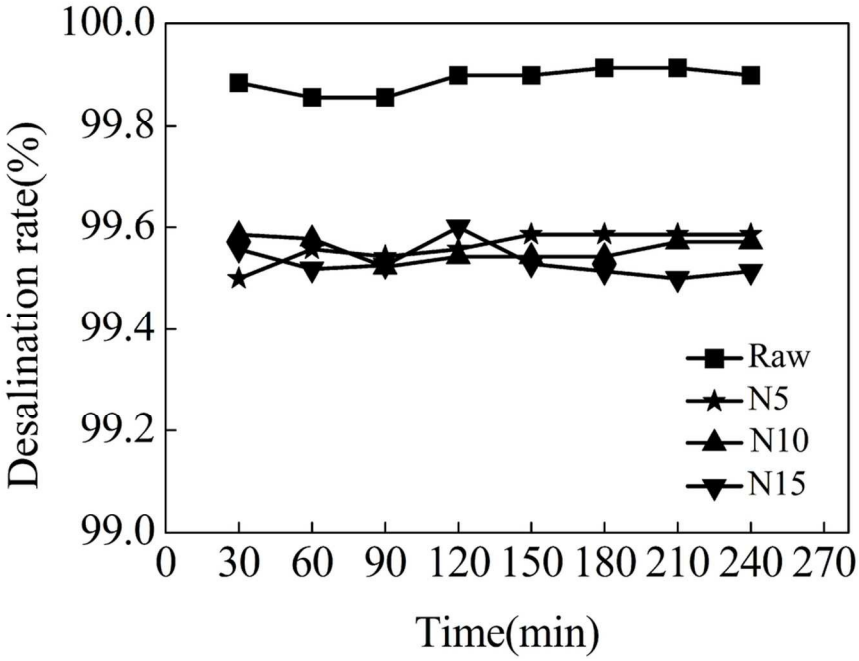

Fig.15
99x78mm (300 x 300 DPI)